Chinese Chemical Letters 35 (2024) 109456

Contents lists available at ScienceDirect

Chinese Chemical Letters

journal homepage: www.elsevier.com/locate/cclet

Neosophoflavonoids A–C, A class of highly oxidized hybrid flavonoids from *Sophora flavescens* with antidiabetic effects

Xu Zhang[1], Jiang Li[1], Kai-Zhou Lu[1], Ya-Nan Yang, Jian-Shuang Jiang, Xiang Yuan, Zi-Ming Feng, Fei Ye*, Pei-Cheng Zhang*

State Key Laboratory of Bioactive Substance and Function of Natural Medicines, Institute of Materia Medica, Chinese Academy of Medical Sciences and Peking Union Medical College, Beijing 100050, China

ARTICLE INFO

Article history:
Received 13 October 2023
Revised 19 December 2023
Accepted 21 December 2023
Available online 26 December 2023

Keywords:
Sophora flavescens
Highly oxidized hybrid flavonoids
Neosophoflavonoids A–C
PTP1B inhibition
Lipid accumulation inhibition

ABSTRACT

Three highly oxidized hybrid flavonoids neosophoflavonoids A–C (**1**, **2a**, and **2b**) were isolated from the roots of *Sophora flavescens*. Neosophoflavonoid A possesses a unique highly oxidized heptacyclic 6/6/6/6/6/6/5 system. Neosophoflavonoids B and C are isomers and share the same highly oxidized hexacyclic 6/6/6/6/6/6 systems. Their planar structures were elucidated from 1D/2D nuclear magnetic resonance (NMR), ultraviolet spectroscopy (UV), infrared spectroscopy (IR), and high resolution electrospray ionization mass spectroscopy (HRESIMS) data. Their absolute configurations were determined by thorough GIAO ^{13}C NMR (DP4+) calculation protocol and electronic circular dichroism (ECD) calculation method. The plausible biosynthetic routes for the compounds were also proposed. All compounds exhibited significant protein tyrosine phosphatase-1B (PTP1B) inhibitory activity with half maximal inhibitory concentration (IC_{50}) values 3.94 ± 0.01, 0.38 ± 0.13, and 0.70 ± 0.01 μmol/L, respectively. In addition, compared to a positive control fenofibrate (Feno) at 20 μmol/L, compounds **2a** and **2b** exhibited stronger inhibitory effects on lipid accumulation in the oleic acid (OA)-induced cell model at 5 and 10 μmol/L.

Sophora flavescens (*S. flavescens*) is well-known species of *Sophora*, and its roots, which are called Kushen in traditional Chinese medicine, are commonly used to treat cancer, skin diseases, and diarrhea [1,2]. To date, a large number of phytochemical studies on *S. flavescens* have been reported and have demonstrated that flavonoids and alkaloids are the major constituents. Among them, approximately 150 flavonoids have been identified, including flavanones, flavanonols, flavonols, chalcones, isoflavones, and biflavonoids [2,3]. Characteristically, the flavonoids usually contain isoprenyl and lavandulyl groups. Pharmacological studies on these reported flavonoids revealed various biological activities, including antidiabetic, anti-inflammatory, antioxidative, antitumor, and antimicrobial activities [2,4–7]. Recently, several unique skeletons derived from flavonoids, such as sophorapterocarside A (a pterocarpine derivative with a unique pterocarpan-glucose-long chain aliphatic acid structure) [8], sophopterocarpan A (a pterocarpine derivative with a benzotetrahydrofuran-fused bicyclo[3.3.1]nonane) [9], and biflavonoids (formed through rare $C_{5'}$-C_{β} or C_3-C_{β} bonds between dihydroflavones and chalcones) [10] were reported. Based on these results, *S. flavescens* possesses structurally intriguing flavonoids and further research on its phytochemistry and biological activity is worthwhile.

During our efforts, three high hybrid flavonoids (neosophoflavonoids A–C, **1**, **2a**, and **2b**) were isolated from the roots of *S. flavescens* (Fig. 1). Compound **1** was characterized by a fantastic heptacyclic 6/6/6/6/6/6/5 skeleton, and compounds **2a**/**2b** were characterized by hexacyclic 6/6/6/6/6/6 skeletons. All compounds were evaluated for their ability to inhibit protein tyrosine phosphatase-1B (PTP1B) and lipid accumulation. Herein, the isolation, structural elucidation, and biological activities of the compounds are described.

Compound **1** was isolated as a pale-yellow powder with ultraviolet spectroscopy (UV) absorption maxima at 204 and 284 nm. Its molecular formula was established as $C_{35}H_{34}O_9$ based on the $[M-H]^-$ ion peak at *m/z* 597.2134 (calcd. for $C_{35}H_{33}O_9$, 597.2130) in the high resolution electrospray ionization mass spectrometry (HRESIMS). The infrared spectroscopy (IR) absorptions of **1** suggested the presence of hydroxyl (3207 cm^{-1}), carbonyl (1791 cm^{-1}), and aromatic rings (1607, 1507, and 1465 cm^{-1}). The ^1H NMR spectrum (Table S3 in Supporting information) presented signals for two ABX aromatic ring systems [δ_H 7.26 (1H, d, J = 8.5 Hz, H-6′), 6.48 (1H, dd, J = 8.5, 2.5 Hz, H-5′), and

* Corresponding authors.
E-mail addresses: yefei@imm.ac.cn (F. Ye), pczhang@imm.ac.cn (P.-C. Zhang).
[1] These authors contributed equally to this work.

https://doi.org/10.1016/j.cclet.2023.109456
1001-8417/

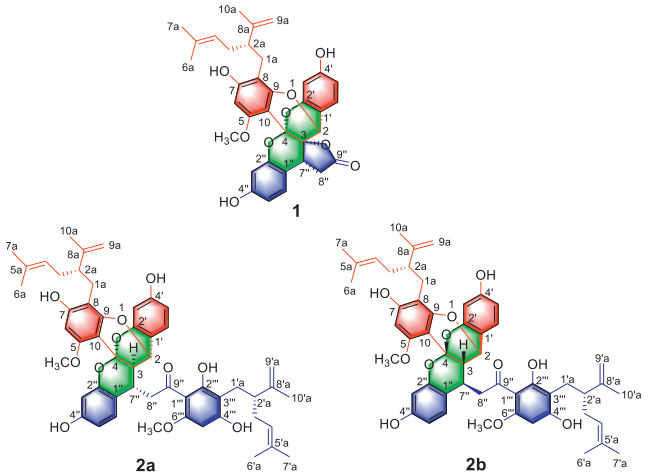

Fig. 1. Chemical structures of compounds **1**, **2a**, and **2b**.

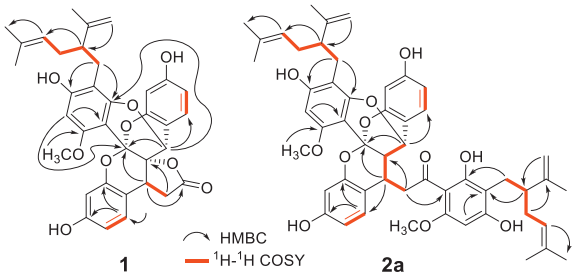

Fig. 2. Key HMBC correlations of **1** and **2a**.

6.34 (1H, d, J = 2.5 Hz, H-3′); 6.89 (1H, d, J = 8.5 Hz, H-6″), 6.46 (1H, dd, J = 8.5, 2.5 Hz, H-5″), and 6.44 (1H, d, J = 2.5 Hz, H-3″)], one penta-substituted aromatic ring [δ_H 5.93 (1H, s, H-6)], one typical lavandulyl group [δ_H 2.49 (2H, m, H-1a), 2.29 (1H, m, H-2a), 1.88 (2H, m, H-3a), 4.86 (1H, m, H-4a), 1.32 (3H, brs, H-6a), 1.56 (3H, brs, H-7a), 4.49 (2H, m, H-9a), and 1.64 (3H, brs, H-10a)], one methylene [δ_H 3.56 (1H, dd, J = 18.0, 9.0 Hz, H-8″a) and 2.56 (1H, brd, J = 18.0 Hz, H-8″b)], two methines [δ_H 5.35 (1H, s, H-2) and 4.06 (1H, d, J = 9.0 Hz, H-7″)], and one methoxyl [δ_H 3.74 (3H, s, 5-OCH$_3$)]. According to the ^{13}C NMR (Table S3) and heteronuclear single quantum coherence (HSQC) spectra, 35 carbon signals were observed including 18 benzene carbons, 10 lavandulyl carbons, one carbonyl carbon (δ_C 176.6), two quaternary carbons (δ_C 78.9 and 98.4), two methine carbons (δ_C 35.8 and 73.1), one methylene carbon (δ_C 38.5), and one methoxyl (δ_C 56.0). The above information suggested that compound **1** possessed the scaffold mode of 15 (flavone) + 10 (lavandulyl) + 9 (phenylpropanoid). In the heteronuclear multiple-bond correlation spectroscopy (HMBC) spectrum (Fig. 2), the correlations of H-1a to C-7/C-9 confirmed that lavandulyl unit was attached at C-8. Additionally, the correlations from H-2 to C-2′/C-6′/C-4/C-9, H-3′ to C-1′, H-6′ to C-4′, and H-6 to C-10/C-8/C-4 suggested the presence of a functionalized flavone moiety. Furthermore, the phenylpropanoid moiety was deduced by the correlations of H-6″ to C-2″/C-4″, H-7″ to C-2″/C-6″/C-9″, and H-8″ to C-1″. Then, these key correlations from H-7″ to C-4 and H-8″ to C-3 revealed that the flavone moiety and phenylpropanoid moiety were linked through C-3/C-7″. The HRESIMS data indicated that compound **1** contained 19 degrees of unsaturation. However, three degrees of unsaturation remained, not including the 16 degrees of unsaturation of flavone, phenylpropanoid, and lavandulyl unit. Herein, the unusual chemical shifts of C-4 (δ_C 98.4) and C-3 (δ_C 78.9) suggested that these two quaternary carbons linked two oxygen atoms and one oxygen atom, respectively. Thus, the challenge was to determine their linkage. According to the chemical shifts of -C=O (δ_C 176.6), a five membered lactone ring was present (the chemical shift of the carbonyl carbon of the six membered lactone was less than 170 ppm) [11,12]. Therefore, the linkages of C-2″-O-C-4, C-2′-O-C-4, and -O=C–O-C-3 were confirmed. Accordingly, the planar structure of **1** was determined to be an unprecedented 6/6/6/6/6/6/5 fused skeleton. According to the correlation of H-2/H-6′ in rotating frame Overhauser effect spectroscopy (ROESY) spectrum and the literature, two pyran rings [C-9→O→C-2→C-3→C-4→C-10] and [C-2′→O→C-4→C-3→C-2→C-1′] were presented through *cis* fusion [11]. Thus, the absolute configuration of **1** possessed the following pairs of potential forms: 2*R**,3*R**,4*R**,7″*S**,2a*R**/2*S**,3*S**,4*S**,7″*R**,2a*S** (I), 2*R**,3*R**,4*R**,7″*S**,2a*S**/2*S**,3*S**,4*S**,7″*R**,2a*R** (II), 2*R**,3*S**,4*R**,7″*R**,2a*R**/2*S**,3*R**,4*S**,7″*S**,2a*S** (III), 2*R**,3*S**,4*R**,7″*R**,2a*S**/2*S**,3*R**,4*S**,7″*S**,2a*R** (IV), 2*R**,3*S**,4*R**,7″*S**,2a*S**/2*S**,3*R**,4*S**,7″*R**,2a*R** (V), 2*R**,3*S**,4*R**,7″*S**,2a*R**/2*S**,3*R**,4*S**,7″*R**,2a*S** (VI), 2*R**,3*R**,4*R**,7″*R**,2a*S**/2*S**,3*S**,4*S**,7″*S**,2a*R** (VII), and 2*R**,3*R**,4*R**,7″*R**,2a*R**/2*S**,3*S**,4*S**,7″*S**,2a*S** (VIII). In the ROESY spectrum, the significant correlation of H-2/H-7″ was observed. However, this correlation cannot be observed in forms V-VIII (Fig. S29 in Supporting information). Herein, GIAO ^{13}C NMR calculations with DP4+ analyses were utilized to differentiate the forms I-IV [13,14]. In order to increase accuracy of the results, two functions and three basis sets were selected to carry out GIAO ^{13}C NMR calculations and DP4+ analyses. As a result, the predicted spectroscopic data for the form IV was in closer agreement with the experimental values (Table S1 in Supporting information). Then, electronic circular dichroism (ECD) calculations were employed to confirm the absolute configuration of **1**. Systematic conformational analyses of the structure of 2*R*,3*S*,4*R*,7″*R*,2a*S* were carried out using molecular mechanics force field MMFF94 calculations. Optimized conformations were obtained at the B3LYP/6–31G(d) level. At the CAM-B3LYP/6–311G(d,p) level, their ECD spectra were calculated using time-dependent density functional theory (TDDFT). The overall calculated ECD spectra were generated by determining their lowest energy conformers through Boltzmann weighting. Throughout the entire range of wavelengths, the calculated spectrum of 2*R*,3*S*,4*R*,7″*R*,2a*S* was consistent with the experimental ECD spectrum of **1** (Fig. 3). Finally, the structure of **1** was established and named neosophoflavonoid A.

As diastereoisomers, compounds **2a** and **2b** were isolated by utilizing a normal-phase chiral column. Herein, only the elucidated process of **2a** is presented. The molecular formula of **2a** was deduced as $C_{52}H_{58}O_{11}$, based on HRESIMS analysis (ion peak at *m/z* 859.4038 $[M+H]^+$, calcd. for $C_{52}H_{59}O_{11}$ 859.4051). The ^{1}H NMR spectrum of **2a** (Table S3) exhibited differences from that of compound **1** as one more penta-substituted aromatic ring [δ_H 6.01 (1H, s, H-5‴)] and one more lavandulyl unit [δ_H 2.66 (2H, brd, J = 7.5 Hz, H-1′a), 2.29 (1H, m, H-2′a), 2.10 (2H, m, H-3′a), 5.06 (1H, m, H-4′a), 1.58 (3H, brs, H-6′a), 1.64 (3H, brs, H-7′a), 4.62 (1H, m, H-9′aa), 4.55 (1H, d, J = 2.5 Hz, H-9′ab), and 1.72 (3H, brs, H-10′a)] were presented. Compared that of compound **1**, the ^{13}C NMR spectrum of **2a** (Table S3) showed 17 more signals that contained six aromatic carbons, ten lavandulyl carbons, and one methoxyl carbon. HMBC correlations from H-8″ to C-1‴, H-5‴ to carbonyl carbon, H-1′a to C-2‴, and H-2′a to C-3‴ suggested that one more penta-substituted aromatic ring was attached at the carbonyl carbon and one more lavandulyl unit was attached at C-3‴ (Fig. 2). In addition, unlike compound **1**, H-3 (δ_H 2.36, 1H, dd, J = 9.5, 2.5 Hz) was presented, indicating that compound **2a** did not contain five-membered lactone ring. Thus, the planar structure of **2a** was established as shown. Similar to **1**, two pyran rings [C-9→O→C-2→C-3→C-4→C-10] and [C-2′→O→C-4→C-3→C-2→C-1′] should be *cis* fused. Then, quantum

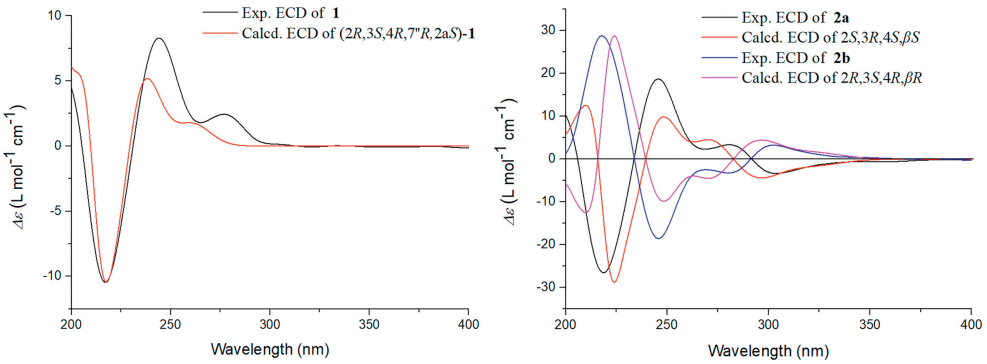

Fig. 3. Experimental ECD and calculated ECD spectra of **1**, **2a**, and **2b**.

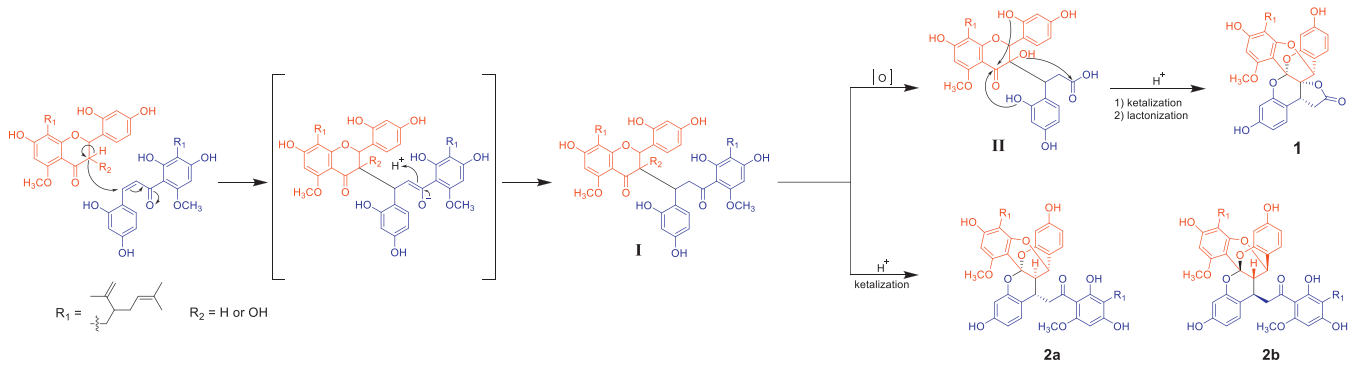

Scheme 1. Proposed biosynthetic pathway for **1**, **2a**, and **2b**.

chemical calculations were used to determine the absolute configurations of compounds **2a** and **2b**. First, considering that two flexible lavandulyl units can produce diverse conformations and have an insignificant influence on the chiral centers, simplified planar structures I-IV (representing eight isomers, as shown in Fig. S37 in Supporting information) were used for the GIAO ^{13}C NMR (DP4+) calculations and ECD calculations. In GIAO ^{13}C NMR calculations, form II corresponded better with the experimental values, which was supported by a DP4+ probability of approximately 99.76% at the B3LYP/6–311G(d,p) level (Fig. S38 in Supporting information). In ECD calculations, 2*S*,3*R*,4*S*,7′′*S* and 2*R*,3*S*,4*R*,7′′*R* were consistent with the experimental ECD spectra of **2a** and **2b**, respectively (Fig. 3). The absolute configurations of C-2a and C-2a′ were determined by deep GIAO ^{13}C NMR calculations and DP4+ analyses. Isomers 2*S*,3*R*,4*S*,7′′*S*,2a*R**,2a′*R**, 2*S*,3*R*,4*S*,7′′*S*,2a*S**,2a′*S**, 2*S*,3*R*,4*S*,7′′*S*,2a*R**,2a′*S**, and 2*S*,3*R*,4*S*,7′′*S*,2a*S**,2a′*R** were calculated for their DP4+ probabilities. Similarly, in order to increase accuracy of the calculation results, two functions and three basis sets were used in process. As results, the 2*S*,3*R*,4*S*,7′′*S*,2a*S**,2a′*R** isomer was the optimal result (Table S2 in Supporting information). Finally, the absolute configurations of **2a** and **2b** were confirmed as 2*S*,3*R*,4*S*,7′′*S*,2a*S*,2a′*R* and 2*R*,3*S*,4*R*,7′′*R*,2a*S*,2a′*R*, respectively. In most reported phytochemical researches on *Sophora flavescens*, the absolute configuration of lavandulyl unit was ambiguous. A few valuable reports assigned the absolute configuration of lavandulyl unit as *S* or *R* according to the X-ray crystallographic analysis or quantum chemical calculations [15,16]. Herein, the thorough quantum calculations unambiguous clarified the absolute configurations of lavandulyl units. Compounds **2a** and **2b** were designated neosophoflavonoid B and neosophoflavonoid C, respectively.

A plausible biosynthetic pathway of **1**, **2a**, and **2b** was presented in Scheme 1. For compound **1**, dimer **I** was generated through a Michael addition reaction between dihydroflavone and chalcone, **II** was formed through the oxidation of **I**. Then, two carbonyls were protonated to form the ketal with the corresponding hydroxyl. Finally, compound **1** was generated by lactonization. The biosynthetic pathways of **2a** and **2b** were similar to that of **1**. For these compounds, **I** was protonated to form the ketal with the corresponding hydroxyl group.

The PTP1B inhibitory effects of all compounds were evaluated *in vitro*. Compound **1** showed moderate inhibitory activity on PTP1B with half maximal inhibitory concentration (IC_{50}) of 3.94 ± 0.01 μmol/L; **2a** and **2b**, however, exhibited stronger inhibitory effects on PTP1B with IC_{50} values of 0.38 ± 0.13 μmol/L and 0.70 ± 0.01 μmol/L (positive control: CCF06240, IC_{50} = 1.73 ± 0.46 μmol/L), respectively. In addition, the cytotoxic activities of compounds **1**, **2a**, and **2b** were evaluated in HepG2 cells by the cell counting kit-8 (CCK-8) assay. During exposure to compounds **1**, **2a**, and **2b** (0.1–20 μmol/L) for 24 h, the viability of HepG2 cells was not significantly affected, showing that the compounds did not exhibit cytotoxicity (Fig. 4). Furthermore, compounds **1**, **2a**, and **2b** exhibited inhibitory effects on lipid accumulation in the oleic acid (OA)-induced cell model in the concentration range of 1–10 μmol/L (Fig. 4), and the inhibitory effects of **2a** and **2b** at 5 and 10 μmol/L were comparable or stronger than those of the positive control fenofibrate (Feno) at a concentration of 20 μmol/L. However, compound **1** at 10 μmol/L only showed a 14.9% inhibitory rate, which was lower than that of the positive control fenofibrate (Feno) at a concentration of 20 μmol/L (26.5%). From the perspective of structure-activity relationship, a multiple substituted aromatic ring with lavandulyl unit in compounds **2a** and **2b** may have an important effect on their inhibitory activities.

In summary, three highly oxidized hybrid flavonoids were isolated from the roots of *Sophora flavescens*. Their absolute configurations were unambiguous clarified by thorough quantum calculations including GIAO ^{13}C NMR (DP4+) calculation protocol and electronic circular dichroism (ECD) calculation method. Additionally, compounds **2a** and **2b** exhibited significant inhibitory effects

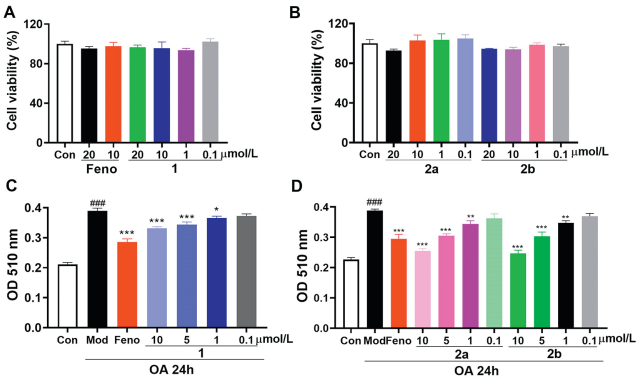

Fig. 4. (A, B) Effects of compounds (Feno, **1**, **2a**, and **2b**) on cell viability of HepG2 cells. (C, D) Compounds alleviated lipid accumulation in OA-induced HepG2 cells, and Oil-red-O staining was used to detect lipid droplets. The results are the mean ± SEM ($n = 6$). $^{###}P < 0.001$ *vs.* control group (Con). $^{*}P < 0.05$, $^{**}P < 0.01$, $^{***}P < 0.001$ *vs.* model group (Mod).

both on PTP1B and lipid accumulation. This investigation furnishes novel and promising structures into the development of antihyperlipidemic candidate.

Declaration of competing interest

The authors declare that they have no known competing financial interests or personal relationships that could have appeared to influence the work reported in this paper.

Acknowledgments

This work was supported by the National Natural Science Foundation of China (No. 81973194) and Biomedical High Performance Computing Platform, Chinese Academy of Medical Sciences.

Supplementary materials

Supplementary material associated with this article can be found, in the online version, at doi:10.1016/j.cclet.2023.109456.

References

[1] D. Luo, X.Y. Dai, H. Tian, et al., Phytomedicine 116 (2023) 154909.
[2] X.R. He, J.C. Fang, L.H. Huang, J.H. Wang, X.Q. Huang, J. Ethnopharmacol. 172 (2015) 10–29.
[3] P. Sun, W.J. Zhao, Q. Wang, et al., Phytomedicine 100 (2022) 154054.
[4] X.Z. Yang, J. Yang, C. Xu, et al., J. Ethnopharmacol. 171 (2015) 161–170.
[5] J.H. Jin, J.S. Kim, S.S. Kang, et al., J. Ethnopharmacol. 127 (2010) 589–595.
[6] J.J. Li, Y. Lin, L. He, et al., Molecules 26 (2021) 7228.
[7] I. Oh, W.Y. Yang, S.C. Chung, et al., Arch. Pharm. Res. 34 (2011) 217–222.
[8] K.Z. Lu, Z.M. Feng, X. Yuan, et al., Chin. J. Chem. 39 (2021) 2763–2768.
[9] H. Zhu, Y.N. Yang, K. Xu, et al., Org. Biomol. Chem. 15 (2017) 5480–5483.
[10] H.W. Yan, H. Zhu, X. Yuan, et al., Bioorg. Chem. 86 (2019) 679–685.
[11] B. Zhou, Y. Alania, M.C. Reis, et al., Org. Lett. 22 (2020) 5304–5308.
[12] X.Z. Sum, A.T. Sneden, Planta Med. 65 (1999) 671–673.
[13] N. Grimblat, M.M. Zanardi, A.M. Sarotti, J. Org. Chem. 80 (2015) 12526–12534.
[14] Y.B. Sun, L.T. Cui, Q.R. Li, et al., Chin. Chem. Lett. 33 (2022) 516–518.
[15] X.B. Huang, L.W. Yuan, J. Shao, et al., Nat. Prod. Res. 35 (2021) 4317–4322.
[16] H. Zhu, Y.N. Yang, Z.M. Feng, J.S. Jiang, P.C. Zhang, Bioorg. Chem. 79 (2018) 122–125.